

First-Principles Search for Half-Metallic Ferromagnetism in Double Perovskite X_2MnUO_6 ($X = Sr$ or Ba) Compounds

S. BERRI^{a,b}

^aLaboratory for Developing New Materials and their Characterizations,
University of Setif 1, Algeria

^bDepartment of Physics, Faculty of Science, University of M'sila, 28000, M'sila, Algeria

Received: 09.06.2020 & Accepted: 06.08.2020

Doi: [10.12693/APhysPolA.138.834](https://doi.org/10.12693/APhysPolA.138.834)

*e-mail: berrisaadi12@yahoo.fr

The structural, electronic and half-metallic properties of X_2MnUO_6 ($X = Sr$ or Ba) are investigated by using the first-principles calculations. It is shown that these two compounds exhibit half-metallic ferromagnetism with an integer magnetic moment of $5.00 \mu_B$. The half-metallicity is attributed by the double-exchange interaction mechanism via the Mn $3d$ -O $2p$ -U $5f$ hybridization. The X_2MnUO_6 compounds are found to be promising candidates for spintronic applications.

topics: X_2MnUO_6 , spintronic, *ab initio* calculations

1. Introduction

Double-perovskite compounds such as $A_2BB'O_6$ have recently received a lot of attention due to their potential applications in numerous industrial and engineering domains [1–5]. The new generation of double perovskites has been widely recognized and deemed technologically promising to be used also in the photovoltaic, photodetector or photocatalytic fields [6–8].

Half-metallic ferromagnetic materials have attracted significant interest of both the academic and industrial circles. Half-metallic ferromagnetism plays an important role in high-performance spintronic applications [9]. These materials have a complete (100%) spin polarization at the Fermi level when one spin channel is metallic while the other channel — a semiconducting one.

Several half-metallic ferromagnetisms have been predicted by first-principles calculations or synthesized experimentally. These include double perovskites (e.g., $CuMn_2InSe_4$ [10] and UX_2O_6 [11]), FC_5N_8 monoclinic [12], Suzuki-type compounds Li_6TMCl_8 [13], double perovskite Sr_2GdReO_6 and $RBaMn_2O_6$ ($X = Nd, Pr, La$) [14, 15] and quaternary Heusler compounds (e.g., $PtZrTiAl$, $PdZrTiAl$, $CoMnCrSb$ and $Ti_2RhSn_{1-x}Si_x$) [16–18].

In this work, a new series of X_2MnUO_6 double perovskites is studied theoretically, where X is the main group element corresponding to Sr or Ba . As opposed to their oxide and halide siblings, polycrystalline oxide perovskites (Sr_2MnUO_6 and Ba_2MnUO_6) have received little attention so far. Only limited data have been reported on the physical properties and thus further studies are needed

on possible spintronic technological applications. This fact has prompted us to investigate the structural, electronic and half-metallic properties of Sr_2MnUO_6 and Ba_2MnUO_6 materials. Our calculations are carried out with the use of first-principles calculations based on the density functional theory within the generalized gradient approximation (GGA) plus the Hubbard parameter U . The results are compared with the experimental and previously published theoretical data, wherever it was possible.

2. Method of calculation

To compute the structural, electronic and half-metallic properties of the X_2MnUO_6 compounds, we have applied the density functional theory (DFT) based on the self-consistent cycle of the full-potential linearized augmented plane wave (FP-LAPW) method [19] into WIEN2k code [20]. The exchange-correlation energy correction is parametrized using the GGA plus Hubbard U term [21]. Surprisingly, this U term is appropriate to improve the band gaps of solids as compared to the GGA and obtain accurate values of the electronic band gaps close to the experimental ones. The Kohn–Sham equations are solved self-consistently using the FP-LAPW method. In the calculations reported here, we use the parameter $R_{MT}K_{max} = 9$ which determines the matrix size (convergence), where K_{max} is the plane wave cut-off and R_{MT} is the smallest of all atomic sphere radii. The radii R_{MT} of the muffin tins (MT) are chosen to be approximately proportional to the corresponding ionic radii. The Mn $3d$ and U $5f$ are treated using the GGA+ U approach. This method

uses an effective parameter $U_{\text{eff}} = U + J$, where U is the Hubbard parameter and J is the exchange parameter. The Hubbard parameter approach, which includes the exchange-correlation potential, is also very efficient for studying strongly correlated electrons, where the energy bandgap of the given material can be evaluated more accurately. Then, for such cases, the core electrons are taken to be relativistic, whereas the valence electrons are considered as semi-relativistic.

These assumptions seem to be best suited for our system and a full potential method. We considered the U_{eff} value to be 6.04 eV and 3.906 eV for U $5f$ and Mn $3d$ atoms, respectively, similarly to [22, 23]. The mesh of k points in the first Brillouin zone relative to the center of Γ point was selected to be $12 \times 12 \times 12$. We have chosen l_{max} and G_{max} to be 10 and 14, respectively.

3. Results and discussion

The atomic structure of the $X_2\text{MnUO}_6$ compounds is known to crystallize in a cubic lattice, which has space group $Fm-3m$ (225), where X atoms occupy $8c(0.25, 0.25, 0.25)$ sites, Mn — $4b(0.5, 0.5, 0.5)$ sites, U — $4a(0, 0, 0)$ sites and O — $24e(0.25, 0, 0)$ sites of the cubic unit cell [24]. The crystal structure of the $X_2\text{MnUO}_6$ alloy is shown in Fig. 1. This compound has been reported to stabilize in a ferromagnetic $Fm-3m$ (225) stable ground state. The experimental lattice parameters have been optimized with Birch–Murnaghan’s [25] equation of state by fitting energy versus cell volume in ferromagnetic (FM) and antiferromagnetic (AFM) cases. The energy minimum was found in the FM together with the stable magnetic configuration, as seen in Fig. 2. The calculated ground state parameters, such as the lattice constant a [Å], bulk modulus B and pressure derivative of the bulk modulus, are shown in Table I. Note that the optimal lattice parameters a obtained by this procedure agree well with the experimental values reported in [24] and with the previous calculations published in [26].

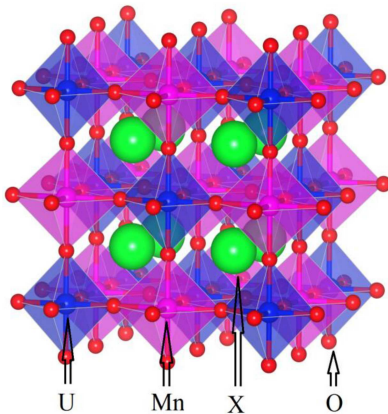


Fig. 1. Crystal structure of $X_2\text{MnUO}_6$.

TABLE I

The calculated bulk parameters of $X_2\text{MnUO}_6$.

Compound	a [Å]	B [GPa]	B'	Ref.
Ba_2MnUO_6	8.501	134.029	4.701	this work
	8.52	—	—	exp. [24]
	8.52	—	—	other [26]
Sr_2MnUO_6	8.379	137.995	3.913	this work
	8.28	—	—	exp. [24]
	8.28	—	—	other [26]

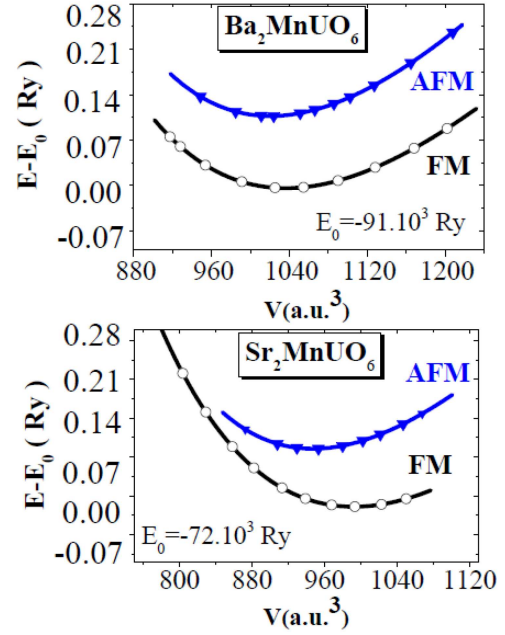


Fig. 2. Calculated normalized energy as a function of volume.

We have also investigated the electronic band structure and total density of states because most of the physical properties of solids are related to those quantities. In the case of the $X_2\text{MnUO}_6$ compound (see Fig. 3), it can be seen that the spin-up direction shows a metallic behaviour and spin-down direction evinces a semiconducting behaviour with an indirect band gap of 3.05 eV and 2.32 eV around the Fermi level for Sr_2MnUO_6 and Ba_2MnUO_6 , respectively. The energy gap in the minority-spin band gap leads to 100% spin polarization at the Fermi level, resulting in the half-metallic behaviour at equilibrium state.

In order to get a deeper insight into the electronic structure of $X_2\text{MnUO}_6$, the partial densities of states (PDOS) have been calculated in both the majority and minority spin (see Fig. 4). The Fermi level was set to zero eV. The density of states was presented for Sr_2MnUO_6 only because in the case of Ba_2MnUO_6 the results are similar, with a small difference. As shown in Fig. 4, the core region (below -16.0 eV) is primarily dominated by X p electrons for both spin channels. The valence region

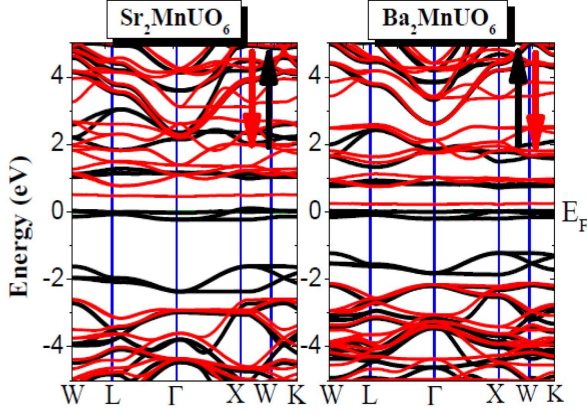


Fig. 3. Band structure for high-symmetry directions in the Brillouin zone. Spin-up (black line) and spin-down (red line).

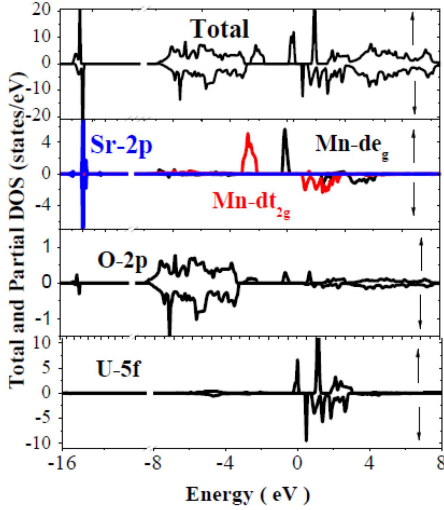


Fig. 4. Total and projected density of states for Sr_2MnUO_6 .

is essentially contributed by the d_{e_g} and $d_{t_{2g}}$ of Mn atoms hybridized with O p and small contribution from U $5f$. The conduction region is mainly contributed by the $5f$ state of U atoms.

The total obtained interstitial and atom-resolved magnetic moments of X_2MnUO_6 are shown in Table II. The total magnetic moments per unit cell of the order of $5.00\mu_B$ for the X_2MnUO_6 alloys are close to integer values and this result confirms the half-metallicity of the considered materials. The basic contribution to the total magnetic moment comes from the Mn and U atoms. Small contributions constitute the interstitial region, whereas the moments of Ba, Sr and O contribute weakly. Our results of the magnetic moment for manganese atoms are in accord with the experimental data reported as $6.2\mu_B$ in [27]. Our results of the magnetic moment for uranium atoms are also in agreement with the previous studies [24]. The presence of the half-metallicity in our compounds is related to the double-exchange mechanism which is a type of

TABLE II

Individual and net magnetic moments m [μ_B] of X_2MnUO_6 compounds.

Compound	m_{Mn}	m_{U}	m_{X}	m_{O}	m_{inter}	m_{tot}
Ba_2MnUO_6	4.133	0.415	0.002	0.016	0.350	5.000
Sr_2MnUO_6	3.902	0.528	0.003	0.027	0.418	5.000

a magnetic exchange that arises between ions in different oxidation states. This theory, first proposed by Zener [28], predicts the relative ease with which an electron may be exchanged between two species and has important implications for whether materials are ferromagnetic or antiferromagnetic. One interaction arises due to the hybridization of Mn $3d$ states with the O $2p$ states and the other interaction arises from the hybridization of U $5f$ states with the O $2p$ states in the Fermi region. The appreciable spin splitting of Mn $3d$ states at the Fermi level also drags the U $5f$ orbitals through the double exchange interactions, i.e., Mn $3d$ -O $2p$ -U $5f$ hybridization.

4. Conclusion

Highly spin-polarized magnetic materials emerge as promising candidates for spintronic technology. We present here a theoretical study of two new double perovskites Ba_2MnUO_6 and Sr_2MnUO_6 in a cubic structure. The half-metallicity is attributed by the double-exchange interaction mechanism via the Mn $3d$ -O $2p$ -U $5f$ hybridization. The X_2MnUO_6 compounds are found to be adequate materials for future spintronic applications.

References

- [1] M.T. Anderson, K.B. Greenwood, G.A. Taylor, K.R. Poeppelmeier, *Prog. Solid State Chem.* **22**, 197 (1993).
- [2] R.P. Borges, R.M. Thomas, C. Cullinan, J.M.D. Coey, R. Suryanarayanan, L. Bendor, L. Pinsard-Gaudart, A. Revcolevschi, *J. Phys. Condens. Matter* **11**, 104 (1999).
- [3] C. Ritter, M.R. Ibarra, L. Morellon, J. Blasco, J. García, J.M. De Teresa, *J. Phys. Condens. Matter* **12**, 8295 (2000).
- [4] S. Berri, *J. Sci. Adv. Mater. Dev.* **5**, 378 (2020).
- [5] Y.-H. Huang, R.I. Dass, Z.-L. Xing, J.B. Goodenough, *Science* **312**, 254 (2006).
- [6] J. Yang, P. Zhang, S.-H. Wei, *J. Phys. Chem. Lett.* **9**, 31 (2018).
- [7] S. Berri, *Chin. J. Phys.* **55**, 2476 (2017).
- [8] G. Garcia-Espejo, D. Rodriguez-Padrón, R. Luque, L. Camacho, G. de Miguel, *Nanoscale* **11**, 16650 (2019).
- [9] R.J. Celotta, D.T. Pierce, *Science* **234**, 333 (1986).

- [10] S. Berri, *J. Supercond. Novel Magn.* **31**, 1941 (2018).
- [11] S. Berri, *J. Sci. Adv. Mater. Dev.* **4**, 319 (2019).
- [12] S. Berri, *Computat. Condens. Matter* **12**, 25 (2017).
- [13] S. Berri, *J. Supercond. Nov. Magn.* **29**, 2381 (2016).
- [14] S. Berri, *J. Magn. Magn. Mater.* **385**, 124 (2015).
- [15] S. Berri, N. Bouarissa, M. Attallah, *J. Supercond. Novel Magn.* **33**, 1737 (2020).
- [16] S. Berri, *Chin. J. Phys.* **55**, 195 (2017).
- [17] S. Berri, *J. Supercond. Nov. Magn.* **29**, 1309 (2016).
- [18] S. Berri, *J. Supercond. Nov. Magn.* **32**, 2219 (2019).
- [19] P. Blaha, K. Schwarz, P. Sorantin, S.B. Trickey, *Comput. Phys. Commun.* **59**, 399 (1990).
- [20] P. Blaha, K. Schwarz, G.K.H. Medsen, D. Kvasnicka, J. Luitz, "WIEN2k: An Augmented Plane Wave plus Local Orbitals Program for Calculating Crystal Properties", Techn. Universität, Wien 2001.
- [21] V.I. Anisimov, J. Zaanen, O.K. Andersen, *Phys. Rev. B* **44**, 943 (1991).
- [22] A. Souidi, S. Bentata, W. Benstaali, B. Bouadjemi, A. Abbad, T. Lantri, *Mater. Sci. Semicond. Process.* **43**, 196 (2016).
- [23] S.A. Khandy, D.C. Gupta, *Int. J. Energy Res.* **44**, 3066 (2020).
- [24] *Structure, Properties and Preparation of Perovskite-Type Compounds*, Ed. F.S. Galasso, Pergamon Press, Oxford 1969 (and references therein).
- [25] F.D. Murnaghan, *Proc. Natl. Acad. Sci. USA* **30**, 244 (1944).
- [26] S. Dimitrovska, S. Aleksovska, I. Kuzmanovski, *Centr. Europ. J. Chem.* **3**, 198 (2005).
- [27] D.G. Franco, R.E. Carbonio, G. Nieva, *IEEE Trans. Magn.* **49**, 4594 (2013).
- [28] C. Zener, *Phys. Rev.* **82**, 403 (1951).